PERGAMON

Available online at www.sciencedirect.com

SCIENCE DIRECT

Acta Astronautica 54 (2003) 69 – 75

ACTA ASTRONAUTICA

www.elsevier.com/locate/actaastro

Academy transactions note

Minimum-time spacecraft maneuver using sliding-mode control☆

Y.W. Jan, J.C. Chiou*

Department of Electrical and Control Engineering, National Chiao-Tung University, Hsinchu 30010, Taiwan, ROC

Received 27 March 2003; accepted 31 March 2003

Abstract

The purpose of this paper is to present a sliding mode control method that can be used to perform a spacecraft large angle maneuver with minimum time. An algorithm of minimum-time SMC is developed to provide the robust tracking control. The simulation results are compared with previous developed control schemes, eigenaxis quaternion regulator, to demonstrate the superiority of the proposed sliding mode control algorithm.

1. Introduction

The major tasks in operating a remote-sensing satellite are to perform rapid multitarget acquisition, pointing, and tracking. The conventional satellite control systems for these tasks are based on a sequence of rotational maneuvers about each control axis to conduct the required three-axis large angle maneuver. The time of such successive rotations is longer (by a factor of 2 or 3) than that of a single maneuver about the eigenaxis that has been known and studied in the last two decades. Among the research, Vadali and Junkins [1] proposed the so-called open-loop schemes for large-angle maneuvers. The open-loop schemes, however, are sensitive to spacecraft parameter uncertainty. Wie et al. [2] chose a linear quaternion feedback regulator with open-loop decoupling control torque for gyroscopic forces to ensure eigenaxis rotations. However, in their approach, the constraints for reaction wheel torque were not considered. The sliding mode control (SMC) is a robust control technique [3] that has applied to the spacecraft attitude-tracking problem by Dwyer and Sira-Ramirez [4], Dwyer and Kim [5], Chen and Lo [6], using the Rodriques parameters as the attitude measurement. Wie et al. [7] proposed a PID saturation control logic to provide a rest-to-rest eigenaxis rotation under slew rate constraint. However, the attitude tracking with minimum time was not considered in their research.

In order to improve the aforementioned drawbacks, an SMC for spacecraft minimum-time tracking maneuver is proposed in this paper. An algorithm of minimum-time SMC is developed to provide the desired tracking trajectories, which are based on an eigenaxis rotation with maximum torques. The eigenaxis rotation with maximum torques eventually provides the minimum-time maneuver. The condition of saturation on wheel torque has been imposed on the control algorithm. Meanwhile, the proposed SMC controller

☆ Endorsed by Jeng-Shing Chern, AIAA, IAA Member (Section 2).

* Corresponding author. Fax: +886-35-715-998.
E-mail address: chiou@cc.nctu.edu.tw (J.C. Chiou).

0094-5765/03/$ - see front matter © 2003 Elsevier Ltd. All rights reserved.
doi:10.1016/S0094-5765(03)00194-2

provides the robust control for removing the effects of model uncertainty.

2. Spacecraft model description

A rigid spacecraft rotating under the influence of body-fixed torquing devices is derived in this section. Reorientation of the spacecraft is accomplished using three reaction wheels that are aligned along three body-fixed control axes. The kinematic and dynamic equations are described by [8]

$$\dot{\bar{q}} = Q\vec{\omega} \tag{1}$$

and

$$\bar{I}\dot{\vec{\omega}} = \vec{L} - \frac{\mathrm{d}\vec{H}_{\mathrm{w}}}{\mathrm{d}t} - \vec{\omega} \times (\bar{I}\vec{\omega} + \vec{H}_{\mathrm{w}}), \tag{2}$$

respectively, where $\vec{L}$ is the external torque, $\vec{\omega} = (\,\omega_1 \quad \omega_2 \quad \omega_3\,)^{\mathrm{T}}$ is the angular rate and $\bar{q} = [\,q_0 \quad q_1 \quad q_2 \quad q_3\,]^{\mathrm{T}}$ denotes the quaternion. The elements of $\bar{q}$ are constrained by

$$\|\bar{q}\| = q_0^2 + q_1^2 + q_2^2 + q_3^2 = 1. \tag{3}$$

Furthermore, Q is an orthogonal matrix of quaternion that can be expressed by the following equation:

$$Q = \frac{1}{2}\begin{bmatrix} -q_1 & -q_2 & -q_3 \\ q_0 & -q_3 & q_2 \\ q_3 & q_0 & -q_1 \\ -q_2 & q_1 & q_0 \end{bmatrix}. \tag{4}$$

The angular momentum of reaction wheels is $\vec{H}_{\mathrm{w}} = \bar{I}_{\mathrm{w}}(\vec{\omega} + \vec{\Omega})$, where $\bar{I}_{\mathrm{w}} = diag(\,I_{\mathrm{w}11} \quad I_{\mathrm{w}22} \quad I_{\mathrm{w}33}\,)$ denotes moment of inertia matrix of the three reaction wheels, and $\vec{\Omega} = \Omega_1\hat{b}_1 + \Omega_2\hat{b}_2 + \Omega_3\hat{b}_3$ is the relative spin rate. In terms of the wheel angular momentum, $\vec{H}_{\mathrm{w}}$, Eq. (2) can be rewritten as

$$\bar{I}\dot{\vec{\omega}} = \vec{L} - \bar{I}_{\mathrm{w}}(\dot{\vec{\omega}} + \dot{\vec{\Omega}}) - \vec{\omega} \times (\bar{I} + \bar{I}_{\mathrm{w}})\vec{\omega} - \vec{\omega} \times \bar{I}_{\mathrm{w}}\vec{\Omega}. \tag{5}$$

The control torque, $\vec{T}$, generated by reaction wheels can be expressed as

$$\vec{T} = \bar{I}_{\mathrm{w}}(\dot{\vec{\omega}} + \dot{\vec{\Omega}}). \tag{6}$$

3. Attitude tracking by SMC

The design procedure of SMC generally contains two fundamental steps.

Step 1: Choose the sliding surface such that the control goal can be achieved. The four quaternions sliding surfaces are chosen as

$$\bar{s} = K(\bar{q} - \bar{q}_{\mathrm{r}}) + (\dot{\bar{q}} - \dot{\bar{q}}_{\mathrm{r}}) = \bar{0} \tag{7}$$

and their time derivatives are given by

$$\dot{\bar{s}} = K(\dot{\bar{q}} - \dot{\bar{q}}_{\mathrm{r}}) + (\ddot{\bar{q}} - \ddot{\bar{q}}_{\mathrm{r}}) = \bar{0}, \tag{8}$$

where $\bar{s} = [\,s_0 \quad s_1 \quad s_2 \quad s_3\,]^{\mathrm{T}}$, $\bar{0} = [\,0 \quad 0 \quad 0 \quad 0\,]^{\mathrm{T}}$, K is a constant and positive definite diagonal matrix, and $\bar{q}_{\mathrm{r}}$ is the reference quaternion trajectory. Note that for the trajectories confined to the surface of Eq. (7),

$$\dot{\bar{q}}_{\mathrm{e}} = -K\bar{q}_{\mathrm{e}}, \tag{9}$$

where $\bar{q}_{\mathrm{e}} = \bar{q} - \bar{q}_{\mathrm{r}}$. The solution of Eq. (9) can be easily obtained as

$$\bar{q}_{\mathrm{e}}(t) = \mathrm{e}^{-Kt}\bar{q}_{\mathrm{e}}(0). \tag{10}$$

This solution shows that the selected sliding surfaces are exponential stable for the reason that K is positive definite.

Step 2: Design the control law such that the reaching and sliding conditions on the sliding surfaces are satisfied. With this in mind, the spacecraft dynamic equations can be expressed in terms of quaternion by taking the time derivative of Eq. (1) and substituting Eq. (5) to obtain

$$\ddot{\bar{q}} = \dot{Q}\vec{\omega} + Q\bar{I}^{-1}(\vec{M} - \vec{T}), \tag{11}$$

where

$$\vec{M} = \vec{L} - \vec{\omega} \times (\bar{I} + \bar{I}_{\mathrm{w}})\vec{\omega} - \vec{\omega} \times \bar{I}_{\mathrm{w}}\vec{\Omega}.$$

The control law for the sliding phase can be found by enforcing $\dot{\bar{s}} = \bar{0}$. Substituting Eq. (8) into Eq. (11), which gives the control law for the reaction wheel torques,

$$\vec{T} = \vec{M} + \bar{I}Q^*\{[K(\dot{\bar{q}} - \dot{\bar{q}}_{\mathrm{r}}) - \ddot{\bar{q}}_{\mathrm{r}} + \dot{Q}\omega] - D \cdot \mathrm{sgn}(\bar{s})\}, \tag{12}$$

where Q^* is the pseudo inverse of Q defined as

$$Q^* = (Q^{\mathrm{T}}Q)^{-1}Q^{\mathrm{T}} = 2\begin{bmatrix} -q_1 & q_0 & q_3 & -q_2 \\ -q_2 & -q_3 & q_0 & q_1 \\ -q_3 & q_2 & -q_1 & q_0 \end{bmatrix}.$$

Matrix D in Eq. (12) is a constant and positive definite diagonal matrix. The discontinuous term has the effect of moving the trajectory back towards the sliding surface when deviations occur resulting from external disturbances or system modeling errors.

In order to demonstrate the stability of the proposed control design, Lyapunov's direct method is used to show that the control law given in Eq. (12) is asymptotically stable for the reaching phase motion. A positive definite candidate Lyapunov function is given by $V = \frac{1}{2}\bar{s}^{\mathrm{T}}\bar{s}$. The requirement for ensuring the reaching and sliding conditions on the sliding surfaces is

$$\dot{V} = \bar{s}^{\mathrm{T}}[K(\dot{\bar{q}} - \dot{\bar{q}}_{\mathrm{r}}) - \ddot{\bar{q}}_{\mathrm{r}} + \dot{Q}\omega + Q\bar{I}^{-1}(\vec{M} - \vec{T})] < 0. \tag{13}$$

Substituting Eq. (12) into Eq. (13) results in a stability constraint of

$$0 > \frac{-\bar{s}^{\mathrm{T}}\{(I - QQ^*)[K(\dot{\bar{q}} - \dot{\bar{q}}_{\mathrm{r}}) - \ddot{\bar{q}}_{\mathrm{r}}] - \overline{\dot{q}q}^{\mathrm{T}}\dot{\bar{q}}\}}{\bar{s}^{\mathrm{T}}QQ^*D\,\mathrm{sgn}(\bar{s})} - 1. \tag{14}$$

The controller design parameters are the values of K and D matrices of Eq. (12). Typical uncertainty arising in spacecrafts during maneuver phase is mainly mass property. Specific constraints on D for the uncertainty of mass property are considered as follows.

The true spacecraft inertia is denoted by

$$\bar{I} = \bar{I}_0 + \Delta\bar{I}, \tag{15}$$

where $\bar{I}_0$ is the measured value of spacecraft inertia, and $\Delta\bar{I}$ is the measurement error. It is assumed that $\Delta\bar{I}$ is sufficiently small such that the zeroth-order term from the binomial expansion of $(\bar{I}_0 + \Delta\bar{I})^{-1}$ is valid. This assumption leads to the following relations:

$$\bar{I}^{-1}\bar{I}_0 \approx I,$$

$$\bar{I}_0^{-1}\Delta\bar{I} \approx 0. \tag{16}$$

Replacing $\bar{I}$ with $\bar{I}_0$ in control law equation (12) results in

$$\vec{T} = \vec{M} + \bar{I}_0 Q^*\{[K(\dot{\bar{q}} - \dot{\bar{q}}_{\mathrm{r}}) - \ddot{\bar{q}}_{\mathrm{r}} + \dot{Q}\omega] - D\,\mathrm{sgn}(\bar{s})\}. \tag{17}$$

Again, performing the calculations analogous to Eqs. (13) and (14), but using Eqs. (16) and (17) yields the constraint relation

$$0 > \frac{-\bar{s}^{\mathrm{T}}\{(I - QQ^*)[K(\dot{\bar{q}} - \dot{\bar{q}}_{\mathrm{r}}) - \ddot{\bar{q}}_{\mathrm{r}}] - \overline{\dot{q}q}^{\mathrm{T}}\dot{\bar{q}}\}}{\bar{s}^{\mathrm{T}}QQ^*D\,\mathrm{sgn}(\bar{s})} - 1 \tag{18}$$

for ensuring closed-loop stability. This constraint is identical to that of the nominal case, where the spacecraft inertia is known exactly.

If larger errors in the inertia matrix exist, then Eq. (16) is not valid and constraint equation (18) should be used with a worst-case estimate of the inertia errors. We assume that the disturbance torque due to the inertia errors on the spacecraft $\vec{L}$ is bounded. This value is unique for a given maneuver. The derivation for the constraint on D to ensure stability is similar to that of Eqs. (13) and (14), where $\vec{L}$ is unknown and therefore not included in control law (12). The time derivative of Lyapunov function V results in a maneuver-dependent constraint similar to Eq. (14)

$$0 > \frac{-\bar{s}^{\mathrm{T}}\{(I - QQ^*)[K(\dot{\bar{q}} - \dot{\bar{q}}_{\mathrm{r}}) - \ddot{\bar{q}}_{\mathrm{r}}] - \overline{\dot{q}q}^{\mathrm{T}}\dot{\bar{q}} + Q\bar{I}^{-1}\vec{L}\}}{\bar{s}^{\mathrm{T}}QQ^*D\,\mathrm{sgn}(\bar{s})} - 1 \tag{19}$$

for ensuring stability.

4. Tracking reference of eigenaxis maneuver with maximum torque

It has been recognized that minimization of the maneuver time around the eigenaxis might be the solution to find the most fast tracking reference. An eigenaxis rotation results in the shortest angular path and, therefore, also in minimum time when the maximum torque is applied. In this section, a minimum-time maneuver trajectory is derived through the concept of applying maximum torque during the eigenaxis maneuver. Firstly, we can express Eq. (12) as

$$\vec{T} = \vec{M} + \vec{N}_{\mathrm{slew}} - \bar{I}Q^*D\,\mathrm{sgn}(\bar{s}). \tag{20}$$

The gyroscopic torque, disturbance torque $\vec{M}$ and the torque needed for on-sliding-phase control, $\bar{I}Q^*D\,\mathrm{sgn}(\bar{s})$, is assumed to be relatively small compared to the slew torque. This assumption is true if the satellite is three-axes stabilized with low reaction wheel momentum before the eigenaxis rotation commences. Note that using a suitable momentum dumping method can ensure this assumption. If we ignore gyroscopic and disturbance torque $\vec{M}$ and accept the fact that the torque needed for on-sliding phase is small. Then by assuming $\bar{I} = diag(\, I_x \quad I_y \quad I_z\,)$, the minimum-time maneuver trajectory can be obtained from the following equations:

$$\bar{I}\dot{\vec{\omega}}_{\mathrm{r}} = \vec{N}_{\mathrm{slew}}, \tag{21}$$

$$\dot{\bar{q}}_{\mathrm{r}} = \frac{1}{2}\begin{bmatrix} -q_{\mathrm{r1}} & -q_{\mathrm{r2}} & -q_{\mathrm{r3}} \\ q_{\mathrm{r0}} & -q_{\mathrm{r3}} & q_{\mathrm{r2}} \\ q_{\mathrm{r3}} & q_{\mathrm{r0}} & -q_{\mathrm{r1}} \\ -q_{\mathrm{r2}} & q_{\mathrm{r1}} & q_{\mathrm{r0}} \end{bmatrix}\vec{\omega}_{\mathrm{r}}. \tag{22}$$

For an eigenaxis slewing, we have

$$\frac{N_{\mathrm{slew},i}}{N_{\mathrm{slew},j}} = \frac{I_i q_{\mathrm{e}i}}{I_j q_{\mathrm{e}j}}, \tag{23}$$

where if

$$i \quad \text{or} \quad j = x,$$
$$i \quad \text{or} \quad j = y,$$
$$i \quad \text{or} \quad j = z,$$

then

$$q_{\mathrm{e}i} \quad \text{or} \quad q_{\mathrm{e}j} = q_{\mathrm{e1}},$$
$$q_{\mathrm{e}i} \quad \text{or} \quad q_{\mathrm{e}j} = q_{\mathrm{e2}},$$
$$q_{\mathrm{e}i} \quad \text{or} \quad q_{\mathrm{e}j} = q_{\mathrm{e3}}.$$

The unique constant ratio properties in Eq. (23) during an eigenaxis rotation can be used to determine the available reaction wheel torque for a minimum time slew. With Eq. (23), the minimum-time slew torque can be written as

$$\vec{N}_{\mathrm{slew}} = \begin{cases} +v\min\limits_i \left|\dfrac{N_{\mathrm{sat}-i}}{I_i q_{\mathrm{e}i}}\right| diag(\bar{I})q_{\mathrm{vec}}, & t \in (0, t_{\mathrm{h}}), \\ -v\min\limits_i \left|\dfrac{N_{\mathrm{sat}-i}}{I_i q_{\mathrm{e}i}}\right| diag(\bar{I})q_{\mathrm{vec}}, & t \in (t_{\mathrm{h}}, 2t_{\mathrm{h}}), \end{cases} \tag{24}$$

where t_{h} is the time to reach halfway mark during slew maneuver, $\vec{\omega}_{\mathrm{r}} = (\,\omega_{\mathrm{r1}} \quad \omega_{\mathrm{r2}} \quad \omega_{\mathrm{r3}}\,)^{\mathrm{T}}, q_{\mathrm{vec}} = [\,q_{\mathrm{e1}}(0) \quad q_{\mathrm{e2}}(0) \quad q_{\mathrm{e3}}(0)\,]^{\mathrm{T}}, \vec{N}_{\mathrm{sat}-i}$ is the saturated wheel torque in body axis i, and $v \in (0,1)$ is the total saturated torque. To satisfy the torque constraint, we have $v < 1$. This is to enable a minimum-time slew while providing a small additional torque for satellite's rotation around eigenaxis. This small additional torque is used to accommodate gyroscopic and disturbance torque $\vec{M}$ and to counteract any perturbations due to modeling errors and external disturbances.

While the slew torque $\vec{N}_{\mathrm{slew}}$ in Eq. (24) used to generate the minimum-time tracking in open loop, the halfway mark is determined using feedback from the error quaternion. The largest error quaternion vector components $[\,q_{\mathrm{err1}}(t) \quad q_{\mathrm{err2}}(t) \quad q_{\mathrm{err3}}(t)\,]$ are compared to its precomputed values at the halfway mark (q_{half}) to determine if the maneuver time reaches t_{h}:

$$\max_i |q_{\mathrm{err}i}(t)| - q_{\mathrm{half}} = \begin{cases} > 0 & \forall t < t_{\mathrm{h}}, \\ < 0 & \forall t > t_{\mathrm{h}}, \end{cases} \tag{25}$$

where

$$\bar{q}_{\mathrm{err}} = \begin{bmatrix} q_{\mathrm{err0}} \\ q_{\mathrm{err1}} \\ q_{\mathrm{err2}} \\ q_{\mathrm{err3}} \end{bmatrix} = \begin{bmatrix} q_{\mathrm{r0}} & q_{\mathrm{r1}} & q_{\mathrm{r2}} & q_{\mathrm{r3}} \\ -q_{\mathrm{r1}} & q_{\mathrm{r0}} & q_{\mathrm{r3}} & -q_{\mathrm{r2}} \\ -q_{\mathrm{r2}} & -q_{\mathrm{r3}} & q_{\mathrm{r0}} & q_{\mathrm{r1}} \\ -q_{\mathrm{r3}} & q_{\mathrm{r2}} & -q_{\mathrm{r1}} & q_{\mathrm{r0}} \end{bmatrix}\begin{bmatrix} q_0 \\ q_1 \\ q_2 \\ q_3 \end{bmatrix}, \tag{26}$$

$$q_{\mathrm{half}} = \frac{\max_i |q_{\mathrm{err}i}(0)|}{|\sin(\phi/2)|}\left|\sin\left(\frac{\phi}{4}\right)\right|. \tag{27}$$

5. Simulation results

In order to demonstrate the superiority of the proposed minimum-time SMC algorithm, we further adapt the eigenaxis quaternion regulator:

$$\vec{T} = \vec{M} + Kq_{\mathrm{vec}} + D\vec{\omega}. \tag{28}$$

It has been shown in Ref. [2] that an eigenaxis rotation will occur when $K = k\,diag(\bar{I})$ and $D = d\,diag(\bar{I})$, where k and d are positive constants.

A typical remote sensing spacecraft system is used as an example. Fig. 1 depicts the remote sensing spacecraft on orbit configuration. The

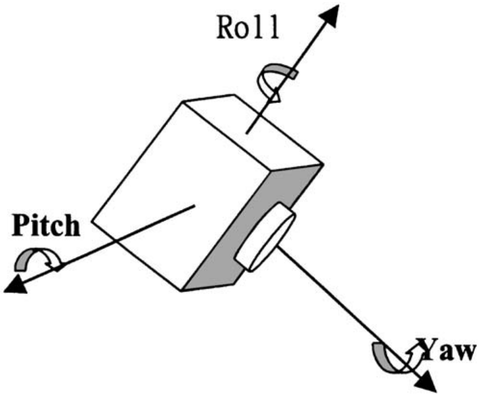

Fig. 1. Experimental spacecraft on-orbit configuration.

Table 1
Initial and final satellite orientation in Euler angles (1–2–3 sequence)

Boundary condition	Roll (deg)	Pitch (deg)	Yaw (deg)
Initial value	0	0	0
Final value	30	45	0

Table 2
Controller parameters

SMC	$W = diag(1, 1, 1, 1)$ $A = diag(0.001, 0.001, 0.001, 0.001)$, $\varepsilon = 0.002, v = 0.9$
Quaternion regulator	$K = diag(3.64, 6.58, 6.72)$, $D = diag(25.5, 46, 47)$

large angle maneuver of interest is specified in terms of Euler angles as shown in Table 1, with $\bar{I} = diag[\,182 \quad 329 \quad 336\,]\,\text{kg}\,\text{m}^2$. The maneuver on yaw is null for the most Earth-pointing remote sensing cases. The configuration of reaction wheels in the simulated spacecraft has been deliberately arranged to accommodate the capability of fast attitude maneuver. According to the wheel configuration, the maximum wheel torque $N_{\text{sat}} = [\,0.56 \quad 0.52 \quad 0.24]$ N m, maximum wheel speed $\Omega_{\max} = 5400$ rpm, and MOI of wheel $I_{\text{w}} = 0.041\ \text{kg}\,\text{m}^2$ are used in the simulation.

In this paper, we assume the nominal inertia matrix is perturbed by 10% and an initial orientation error of 2°. Control parameters for all simulation cases are listed in Table 2. Because of the existence of nonideality in the practical implementation of $\text{sgn}(\bar{s})$, the control law in Eq. (12) generally suffers from the chattering problem. To alleviate such undesirable performance, the sign function is modified as

$$sat(s_i, \varepsilon) = \begin{cases} 1 & s_i > \varepsilon, \\ s_i & |s_i| \leqslant \varepsilon \qquad i = 0, 1, 2, 3. \\ -1 & s_i < -\varepsilon, \end{cases} \quad (29)$$

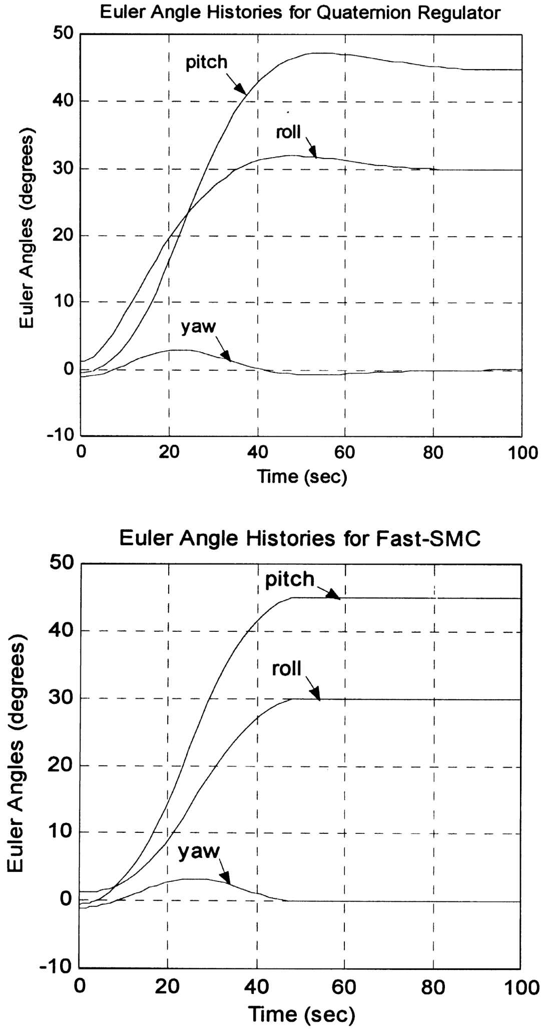

Fig. 2. Euler angles for large-angle slew.

The simulation has been carried out by using Matlab/Simulink software with 100 s simulation time. Fig. 2 shows a large angular rotation with the corresponding roll, pitch and yaw angles during the

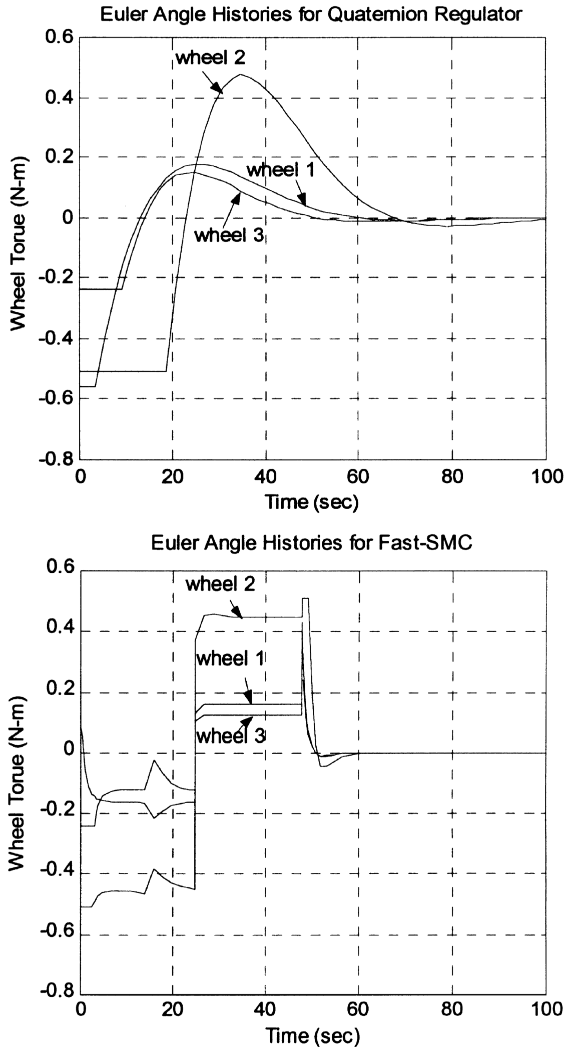

Fig. 3. Reaction wheels torques during large-angle slew.

maneuvers. The proposed SMC algorithm precedes the quaternion regulator with respect to the slew time and pointing accuracy. Compared to the proposed SMC algorithm, the quaternion regulator is not inherently time optimal. In Fig. 3, the corresponding reaction wheel torques for two cases have been obtained. At the beginning of the slewing, we observe that the quaternion regulator produced a maximum constant wheel torque constraint of $N_{sat} = [\,0.56 \quad 0.52 \quad 0.24\,]$ N m. The proposed SMC algorithm satisfies the torque constraint by using

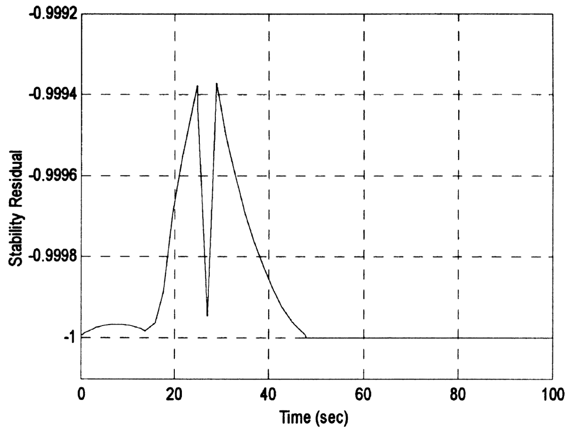

Fig. 4. Stability constraint residual for the fast-SMC maneuver (must be negative for stability as described in Eq. (14)).

0.468 N m on pitch axis with $v = 0.9$ as the upper limit. Therefore, they provide 0.052 N m for the additional small torques. The maximum wheel speed is much lower than the speed limit of 5400 rpm given by hardware capability. Fig. 4 demonstrates the satisfaction of stability constraint, given in Eq. (14) that must be negative. This result verified the control law design of SMC where closed-loop stability has been ensured.

6. Conclusions

An algorithm of minimum-time SMC to perform fast large-angle maneuvers is proposed for a three-axis reaction wheel control of spacecraft. An eigenaxis rotation with maximum torques has been used to determine the tracking reference for the proposed SMC tracking control. The maneuver time of the proposed minimum-time SMC control is much faster (by a factor of 2 or 3) than the conventional approach that is based on a sequence of rotational maneuvers about each control axis to conduct the required three-axis large-angle maneuver. Compared to the quaternion regulator obtained from simulation optimization, the minimum-time SMC has been demonstrated to improve the slew time performance for the experimental target rotation of a typical small remote sensing satellite. Moreover, robustness against inertia modeling errors is ensured by tracking the reference maneuver.

References

[1] S.R. Vadali, J.L. Junkins, Spacecraft large angle rotational maneuvers with optimal momentum transfer, Journal of the Astronautical Sciences 31 (1983) 217–235.
[2] B. Wie, H. Weiss, A. Aropostathis, Quaternion feedback regulator for spacecraft eigenaxis rotations, Journal of Guidance, Control, and Dynamics 12(3) (1989) 375–380.
[3] V.I. Utikin, Sliding Modes and Their Application to Variable Structure System, MIR Publishers, Moscow, Russia, 1978.
[4] T.A.W. Dwyer, H. Sira-Ramirez, Variable-structure control of spacecraft attitude maneuvers, Journal of Guidance, Control, and Dynamics 11(3) (1988) 262–270.
[5] T.A.W. Dwyer, J. Kim, Bandwidth-limited robust nonlinear sliding control of pointing and tracking maneuvers, Proceedings of 1989 American Control Conference, Vol.2, American Automatic Control Council, 1989, pp. 1131–1135.
[6] S.C. Lo, Y.P. Chen, Smooth sliding-mode control for spacecraft attitude tracking maneuvers, Journal of Guidance, Control, and Dynamics 18(6) (1995) 1345–1349.
[7] B. Wie, D. Bailey, C. Heiberg, Rapid multitarget acquisition and pointing control of agile spacecraft, Journal of Guidance, Control, and Dynamics 25(1) (2002) 96–104.
[8] J.R. Wertz, Spacecraft Attitude Determination and Control, Reidel, Dordrecht, The Netherlands, 1980 (Chapters 12, 16).